

Preparation and Reactivity of Pendent $-\text{CO}_2\text{Rh}^{\text{III}}(\text{phthalocyanine})$ Bound to a Poly(acrylate) Backbone. Effects of the Hypercoiled Backbone on the Association, Photochemical, and Thermal Redox Reactions of the Pendent Macrocycle

S. Thomas, G. Ruiz, and G. Ferraudi*

Radiation Laboratory, Notre Dame, Indiana 46556-0579

Received June 7, 2006; Revised Manuscript Received July 19, 2006

ABSTRACT: Poly(acrylate) was derivatized with $\text{Rh}^{\text{III}}(\text{pc})$ (pc = phthalocyanine) and the morphology of the strands was established by AFM microscopy. The strands of the polymer, poly- $\text{Rh}^{\text{III}}(\text{pc})$, were seen as the strings of spherules expected for an hypercoiled poly(acrylate) backbone. Phthalocyanine pendants in a polymer, poly- $\text{Rh}^{\text{III}}(\text{pc})$, having a 1:8 stoichiometric relationship of $-\text{Rh}^{\text{III}}(\text{pc})$ to $-\text{CH}_2\text{CH}(\text{CO}_2-)-$ exhibited chemical properties different from those communicated for $\text{Rh}^{\text{III}}(\text{pc-tetrasulfonate})^{3-}$ in aqueous medium or $\text{XRh}^{\text{III}}(\text{pc})$, X = Cl, Br, I, in nonaqueous media. Reactions of poly- $\text{Rh}^{\text{III}}(\text{pc})$ with reducing radicals like a e^-_{aq} , $(\text{CH}_3)_2\text{C}^{\bullet}\text{OH}$, NiL^+ (L = [14]aneN₄, $\text{Me}_6[14]\text{aneN}_4$), or oxidants, i.e., N_3^{\bullet} , Cl_2^+ , Br_2^+ , or NiL^{3+} were investigated with the pulse radiolysis technique. The phthalocyanine radicals formed in these redox reactions were characterized by means of the transient UV–vis spectrum, and the kinetics of the formation and decay of the radicals were followed at various wavelengths. The photophysical and photochemical processes of poly- $\text{Rh}^{\text{III}}(\text{pc})$ were studied by laser flash photolysis. The lifetime of the excited state, $t = 133$ ns, correlates well with the slow component of the decay of the luminescence detected in the NIR region. This transient has been assigned to a ligand field, LF, excited-state not observed in previous works when $\text{XRh}^{\text{III}}(\text{pc})$ complexes were irradiated in homogeneous solution. The thermal and photochemical properties of poly- $\text{Rh}^{\text{III}}(\text{pc})$ are discussed on the basis of environmental conditions affecting the pendent macrocycles in the strand of polymer.

Introduction

The study of the chemical properties of metalated and metal-free phthalocyanines remains a very active field of research. Application of the phthalocyanines to numerous fields of chemistry has motivated the interest in these compounds.^{1–28} Among these many applications is the catalysis of various reactions in homogeneous solution and heterogeneous phase with transition metal phthalocyanines grafted to organic polymers. Aside the polymerization of pendent groups in a ligand of the complex,²⁹ the grafting of phthalocyanine and other transition metal complexes into polymers has been based in two general strategies.^{23,24,28} They respectively involve the coordination of transition metal complexes through the metal ion to pendent ligands of a polymer backbone or linking one ligand by covalent bonds to a polymer backbone. In the former strategy, metal ions are inert to ligand substitution, e.g., Co^{III} , allowing the complex to be irreversibly fastened to ligands in the polymer. The inertness toward ligand substitution suppresses the detachment of the transition metal complex from the strand of polymer and its migration to the bulk of the solution. On this basis, Rh^{III} was expected to be a convenient metal center for the coordination of the phthalocyanine to a polymer backbone.

Previous studies have shown that monomeric $\text{XRh}^{\text{III}}(\text{pc})$ complexes (pc = phthalocyanine; X = Cl, Br, I) are inert with regard to the thermal substitution of the ligand X^- .^{25,26} In addition, the redox chemistry of the $\text{XRh}^{\text{III}}(\text{pc})$ could be used for the catalysis of processes in homogeneous solution.²⁵ The redox potential of the couples $\text{XRh}^{\text{III}}(\text{pc})/\text{XRh}^{\text{II}}(\text{pc})$ and $\text{XRh}^{\text{IV}}(\text{pc})/\text{XRh}^{\text{III}}(\text{pc})$ greatly disfavors changes of the metal center's oxidation state.^{27,28} Thermal or photochemical redox reactions of $\text{XRh}^{\text{III}}(\text{pc})$ are therefore mediated by $\text{XRh}^{\text{III}}(\text{pc}^{\bullet\pm})$ ligand

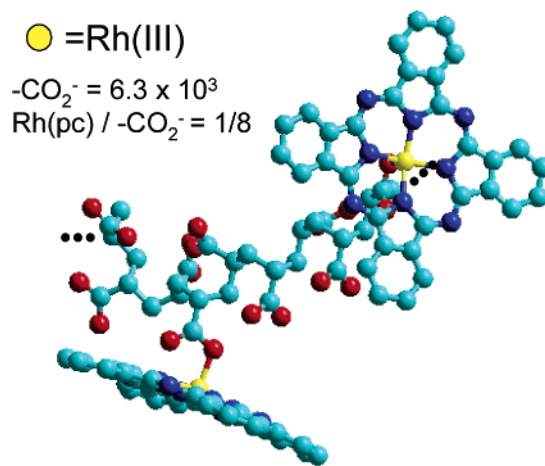


Figure 1. Model showing the average distribution of isolated $\text{Rh}^{\text{III}}(\text{pc})^+$ groups in a short segment of poly($\text{Rh}^{\text{III}}(\text{pc})$). To simplify the presentation, no hydrogen atoms and dimers are shown in the structure. The total number of $-\text{CO}_2-$ groups and the ratio of $\text{Rh}^{\text{III}}(\text{pc})^+$ to $-\text{CO}_2-$ groups in the strand are indicated in the figure.

radical species. Nevertheless trace concentrations of $\text{XRh}^{\text{II}}(\text{pc})^-$, formed after a photoinduced hydrogen abstraction from an organic solvent, accelerate the substitution of the ligand X^- .

When coordination complexes are hosted by a poly(anion), electrostatic interactions and environmental conditions created by the poly(anion) can change photochemical and thermal reactions of the complexes grafted in the polymer. In this work, the incorporation of $-\text{Rh}^{\text{III}}(\text{pc})$ in poly(acrylate), Figure 1, has been investigated as a mean to place the phthalocyanine in aqueous solution and to change the thermal and photochemical reactions of the $-\text{Rh}^{\text{III}}(\text{pc})$ group.

* Corresponding author. E-mail: Ferraudi.1@nd.edu.

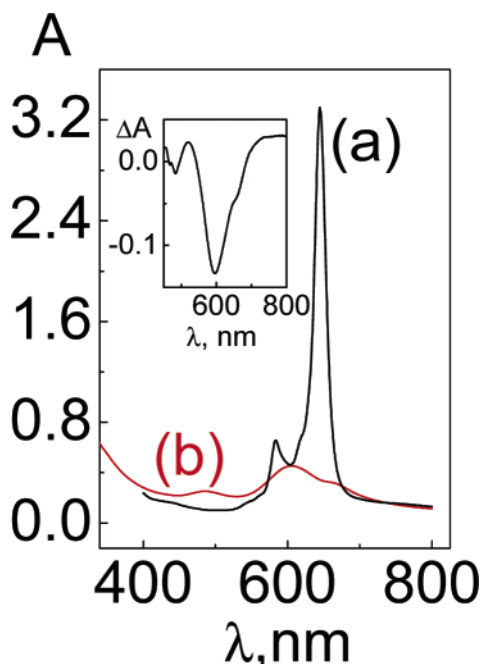


Figure 2. Spectra of monomeric $\text{HSO}_4\text{Rh}^{\text{III}}(\text{pc})$ (a) and $\text{poly-Rh}^{\text{III}}(\text{pc})$ (b) in solutions containing 5×10^{-5} M $\text{Rh}(\text{III})$ chromophores. The inset shows the difference spectrum of two solutions of $\text{poly-Rh}^{\text{III}}(\text{pc})$, 5×10^{-5} M in $-\text{CO}_2\text{Rh}^{\text{III}}(\text{pc})$ chromophores. The spectrum of one solution was subtracted from the spectrum of another containing 10^{-2} M UO_2^{2+} in addition to the $\text{poly-Rh}^{\text{III}}(\text{pc})$.

units, $-\text{CH}_2\text{CH}(\text{CO}_2^-)-$, were in general too insoluble in aqueous media and their properties were not investigated. In contrast to these compounds, those with loads equal to or smaller than 1:10 exhibited good solubilities in aqueous media. Phthalocyanine pendants in a polymer with a 1:8 stoichiometric relationship of $-\text{Rh}^{\text{III}}(\text{pc})$ to $-\text{CH}_2\text{CH}(\text{CO}_2^-)-$ exhibited chemical properties different of the $\text{Rh}^{\text{III}}(\text{tspc})^{3-}$ in aqueous medium or the $\text{XRh}^{\text{III}}(\text{pc})$, $\text{X} = \text{Cl}, \text{Br}, \text{I}$, in nonaqueous media. The properties of this particular polymer, named $\text{poly-Rh}^{\text{III}}(\text{pc})$, are described next.

Stacking of $-\text{CO}_2\text{Rh}^{\text{III}}(\text{pc})$. A less intense and somehow broader Q-band than in the spectrum of $\text{HSO}_4\text{Rh}^{\text{III}}(\text{pc})$ is seen in the spectrum of $\text{poly-Rh}^{\text{III}}(\text{pc})$, Figure 2. The $\text{Rh}^{\text{III}}(\text{tspc})^{3-}$ spectrum in aqueous solution shows an intense absorption band at ~ 640 nm, i.e., the Q-band of the phthalocyanine ligand.²⁷ It is assigned to the 0–0 vibronic transition from the ^1A ground state to the first $^1\pi\pi^*$ excited state, Figure 2a. Other vibronic components of the band are seen at shorter wavelengths. In metallophthalocyanines, the broadening of the Q-band has been associated with the stacking of metallophthalocyanines in dimers containing two or more units of the macrocyclic complex. The broad Q-band observed in the spectrum of $\text{poly-Rh}^{\text{III}}(\text{pc})$ must also be associated with a stacking of metallophthalocyanine pendants. Given the reduced load of $-\text{Rh}^{\text{III}}(\text{pc})$ and limits to the flexibility of the backbone, only the dimers are probably formed by the π stacking of two phthalocyanine pendants. Further evidence of the $-\text{CO}_2\text{Rh}^{\text{III}}(\text{pc})$ stacking in $\text{poly-Rh}^{\text{III}}(\text{pc})$ was provided by changes in the Q-band of $\text{poly-Rh}^{\text{III}}(\text{pc})$ UV–vis when aqueous solutions of the polymer contained metal ions, e.g., UO_2^{2+} , capable of forming complexes with carboxylates. A decrease in the intensity of the Q-band, inset to Figure 2, shows that the stacking of $-\text{CO}_2\text{Rh}^{\text{III}}(\text{pc})$ pendants in the polymer strand increases when UO_2^{2+} is complexed by free carboxylate groups. Comparisons were made between the spectra of solutions having the same ionic strength, $I = 10^{-3}$ M, adjusted with NaClO_4 . Changes in the UV–vis spectrum of

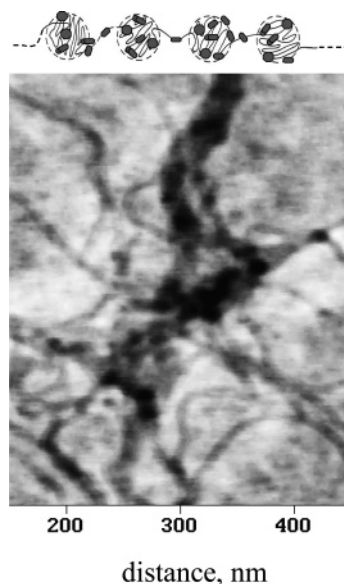


Figure 3. Typical AFM image of $\text{poly-Rh}^{\text{III}}(\text{pc})$ showing strings of spherules, bottom. The sample was prepared with a procedure described elsewhere in the text from a solution containing 2.5×10^{-8} M strands of $\text{poly-Rh}^{\text{III}}(\text{pc})$. The data scale is 4.0 nm. The approximate distribution of $-\text{CO}_2\text{Rh}^{\text{III}}(\text{pc})$ pendants, blue circles, in the hypercoiled strand are shown in the top figure.

$\text{poly-Rh}^{\text{III}}(\text{pc})$ were also induced with 10^{-5} – 10^{-4} M $\text{Ni}(\text{II})$ macrocyclic complexes a, b, or c. Changes in the spectrum of $\text{poly-Rh}^{\text{III}}(\text{pc})$ caused by any of these $\text{Ni}(\text{II})$ complexes bear a strong resemblance to those observed in the presence of UO_2^{2+} .

In comparing this behavior to the behavior of the metallophthalocyanines in solution phase, the stacking of the $-\text{CO}_2\text{Rh}^{\text{III}}(\text{pc})$ pendants demands large concentrations of the pendant in the strand of $\text{poly-Rh}^{\text{III}}(\text{pc})$. Because of the low load of $-\text{CO}_2\text{Rh}^{\text{III}}(\text{pc})$ in $\text{poly-Rh}^{\text{III}}(\text{pc})$, a particular morphology of the strand is necessary to cause the high concentration of pendants.

Strand Morphology. The morphology of the polymer strands was investigated in an AFM microscope in the tapping mode. A string of spherules was observed in samples prepared with different procedures, Figure 3. These strings of spherules indicated the hypercoiling of the poly(acrylate) backbone in a manner resembling the hypercoiled poly(metaacrylate).^{36,37}

Reactivity of $\text{Poly-Rh}^{\text{III}}(\text{pc})$ with Radicals. The spectroscopy of the products formed when reductants, i.e., e^-_{aq} or $(\text{CH}_3)_2\text{C}^\bullet\text{OH}$, NiL^+ ($\text{L} = [14]\text{aneN}_4$, $\text{Me}_6[14]\text{aneN}_4$), or oxidants, i.e., N_3^\bullet , $\text{Cl}_2^{\bullet-}$, $\text{Br}_2^{\bullet-}$, or NiL^{3+} , react with $\text{poly-Rh}^{\text{III}}(\text{pc})$ and the kinetics of the products formation were investigated with the technique of pulse radiolysis. Transient absorption spectra resulting from the oxidation of $\text{poly-Rh}^{\text{III}}(\text{pc})$ by N_3^\bullet , $\text{Cl}_2^{\bullet-}$, or $\text{Br}_2^{\bullet-}$ were recorded with solutions of $\text{poly-Rh}^{\text{III}}(\text{pc})$ having $\sim 10^{-4}$ M $-\text{CO}_2\text{Rh}^{\text{III}}(\text{pc})$ chromophores and 0.1 M Cl^- , 0.1 M N_3^- , or 0.05 M Br^- . The reactions of these oxidants produce a bleach of the Q-band in the near-IR and a broad absorption band with a maximum at ~ 500 nm, Figure 4. This spectrum is similar to the literature spectrum of $\text{ClRh}^{\text{III}}(\text{pc}^+)$ and it has been attributed to the formation of $-\text{CO}_2\text{Rh}^{\text{III}}(\text{pc}^+)$ chromophores.²⁷

The kinetics of the $\text{poly-Rh}^{\text{III}}(\text{pc})$ oxidation by N_3^\bullet radicals was investigated at $I_{\text{ob}} = 500$ nm where the difference spectrum of $-\text{CO}_2\text{Rh}^{\text{III}}(\text{pc}^+)$ chromophores exhibits a maximum. The oscillographic traces used for the calculation of the rate constant were obtained by radiolyzing N_2O saturated solutions of $\text{poly-Rh}^{\text{III}}(\text{pc})$ containing 2.9×10^{-5} M to 2.4×10^{-4} M

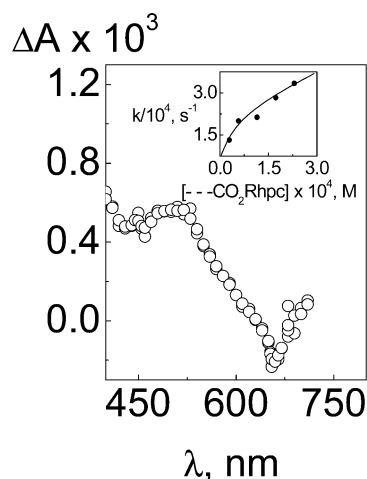


Figure 4. Transient absorption spectrum of $--\text{CO}_2\text{Rh}^{\text{III}}(\text{pc}^{\bullet+})$ radicals in the strand of polymer. The radicals were formed when poly- $\text{Rh}^{\text{III}}(\text{pc})$ was oxidized by pulse radiolytically generated N_3^{\bullet} radicals. In this experiment, N_2O -saturated solutions of poly- $\text{Rh}^{\text{III}}(\text{pc})$, 1.0×10^{-4} M in $--\text{CO}_2\text{Rh}^{\text{III}}(\text{pc})$ chromophores, contained 0.1 M NaN_3 . The inset shows the dependence of the $--\text{CO}_2\text{Rh}^{\text{III}}(\text{pc}^{\bullet+})$ radical formation rate constant on the $--\text{CO}_2\text{Rh}^{\text{III}}(\text{pc})$ concentration.

$--\text{CO}_2\text{Rh}^{\text{III}}(\text{pc})$ with an ionic strength, $I = 0.1$ M, adjusted with NaN_3 , Figure 4. A nonlinear dependence of the rate constant with the concentration of chromophores was ascribed to poly- $\text{Rh}^{\text{III}}(\text{pc})$ concentration-dependent changes in the $--\text{CO}_2\text{Rh}^{\text{III}}(\text{pc})$ stacking within the strand.

The oxidation of poly- $\text{Rh}^{\text{III}}(\text{pc})$ by $\text{Ni}(\text{III})$ macrocyclic complexes, is markedly different of the reactions with N_3^{\bullet} , $\text{Cl}_2^{\bullet-}$, or $\text{Br}_2^{\bullet-}$ described above. Solutions containing 0.1 M Cl^- , 10^{-2} M NiL^{2+} , and 2.4×10^{-4} M $--\text{CO}_2\text{Rh}^{\text{III}}(\text{pc})$ were saturated with N_2O and pulse radiolyzed. The rapid growth of the NiL^{3+} spectrum was observed on a time scale $t < 400$ ns, Figure 5a. The formation of the $\text{Ni}(\text{III})$ products occurs with a pseudo first-order kinetics. Second-order rate constants, $k = 1.2 \times 10^9 \text{ M}^{-1} \text{ s}^{-1}$ for $\text{L} = \text{Me}_6[14]\text{janeN}_4$ and $k = 2.4 \times 10^9 \text{ M}^{-1} \text{ s}^{-1}$ for $\text{L} = [14]\text{janeN}_4$, were calculated from the rate constants obtained under the pseudo first-order kinetics. Further spectral changes took place in a time scale $t > 400$ ns due to the reaction of the NiL^{3+} complexes with $--\text{CO}_2\text{Rh}^{\text{III}}(\text{pc})$ chromophores of the poly- $\text{Rh}^{\text{III}}(\text{pc})$, Figure 5b. A recovery of the solution's absorbance at wavelengths of the Q-band and an absorption band, $\lambda_{\text{max}} = 530$ nm, were observed at the end of the reaction. The rate of the spectral changes exhibited a first-order kinetics and the rate constant of the process, $k = 4.4 \times 10^6 \text{ s}^{-1}$, was independent of λ_{ob} between 450 and 600 nm. Similar spectral changes were observed when solutions containing 0.1 M Cl^- , 10^{-2} M NiL^{2+} , and 2.4×10^{-4} M $\text{Rh}^{\text{III}}(\text{tspc})^{3-}$ were saturated with N_2O and pulse radiolyzed. However, the oxidation of NiL^{2+} was faster, $k \sim 10^{10} \text{ M}^{-1} \text{ s}^{-1}$, and the formation of the adduct was slower, $k = 10^5 \text{ s}^{-1}$, than that in the presence of poly- $\text{Rh}^{\text{III}}(\text{pc})$.

In contrast to the facile oxidation of $--\text{CO}_2\text{Rh}^{\text{III}}(\text{pc})$ chromophores by the above-mentioned radicals, poly- $\text{Rh}^{\text{III}}(\text{pc})$ proved to be more discriminative toward electron donors. Neither e_{aq}^- nor NiL^+ macrocyclic complexes were observed to react with solutions of poly- $\text{Rh}^{\text{III}}(\text{pc})$ where the concentration of $--\text{CO}_2\text{Rh}^{\text{III}}(\text{pc})$ chromophores was equal to or less than 2.4×10^{-4} M. However, the spectrum of the reduced chromophore $--\text{CO}_2\text{Rh}^{\text{III}}(\text{pc}^{\bullet-})$, similar to the literature spectrum of $\text{ClRh}^{\text{III}}(\text{pc}^{\bullet-})$, was observed when N_2O saturated solutions of poly- $\text{Rh}^{\text{III}}(\text{pc})$, 2.4×10^{-4} M in $--\text{CO}_2\text{Rh}^{\text{III}}(\text{pc})$ chromophores, reacted with pulse radiolytically generated $(\text{CH}_3)_2\text{C}^{\bullet}\text{OH}$ radicals.

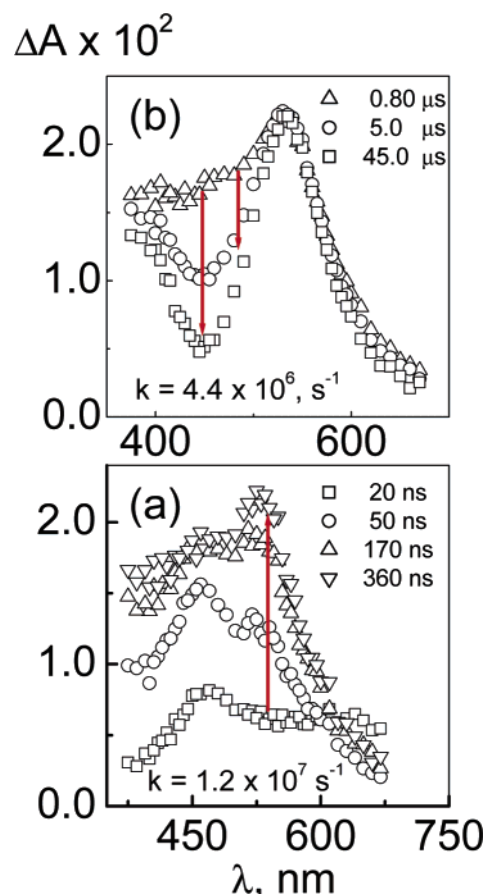
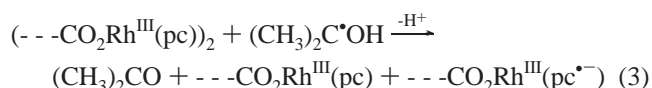
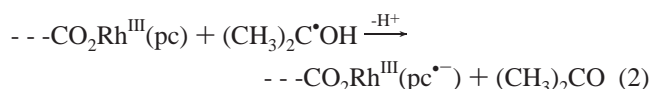


Figure 5. Transient spectra recorded when pulse radiolytically generated $\text{Ni}^{\text{III}}(\text{Me}_6[14]\text{dieneN}_4)\text{Cl}_2^{2+}$ reacted with poly- $\text{Rh}^{\text{III}}(\text{pc})$. The N_2O -saturated solution was 0.1 M in Cl^- and it also contained 10^{-3} M $\text{Ni}^{\text{III}}(\text{Me}_6[14]\text{dieneN}_4)^{2+}$ and a concentration of poly- $\text{Rh}^{\text{III}}(\text{pc})$ equivalent to 1.0×10^{-4} M $--\text{CO}_2\text{Rh}^{\text{III}}(\text{pc})$ chromophores.

An overall rate constant, $k = 7.5 \times 10^9 \text{ M}^{-1} \text{ s}^{-1}$, was calculated for the reaction of $(\text{CH}_3)_2\text{C}^{\bullet}\text{OH}$ radicals with poly- $\text{Rh}^{\text{III}}(\text{pc})$ monomeric pendants, $--\text{CO}_2\text{Rh}^{\text{III}}(\text{pc})$, and dimeric pendants, $(--\text{CO}_2\text{Rh}^{\text{III}}(\text{pc}))_2$, eqs 2 and 3.



Photophysical and Photochemical Processes. Deaerated solutions of poly- $\text{Rh}^{\text{III}}(\text{pc})$, 2.4×10^{-4} M in $--\text{CO}_2\text{Rh}^{\text{III}}(\text{pc})$ pendants, were flash irradiated at 351 nm. The irradiation produced a transient absorption spectrum with a broad band centered at ~ 500 nm, Figure 6. The decay of the spectrum was monitored at several wavelengths, $\lambda_{\text{ob}} = 450, 500$, and 550 nm. Oscillographic traces collected at these wavelengths showed the same rate of decay. A rate constant, $k = 7.5 \times 10^6 \text{ s}^{-1}$, was calculated from the lifetime, $\tau = 133$ ns, of the absorbance decay. To correlate these transients to excited-state processes, the poly- $\text{Rh}^{\text{III}}(\text{pc})$ luminescence was investigated with a solution of the polymer, 2.4×10^{-5} M in $--\text{CO}_2\text{Rh}^{\text{III}}(\text{pc})$ pendants, irradiated at 337 nm. The decay of the luminescence exhibited two components, one faster than the other. A slow component of the emission decay was detected in the NIR region. The lifetime of the NIR emission was approximately the same, $\tau = 140$ ns, communicated above for the decay of the transient

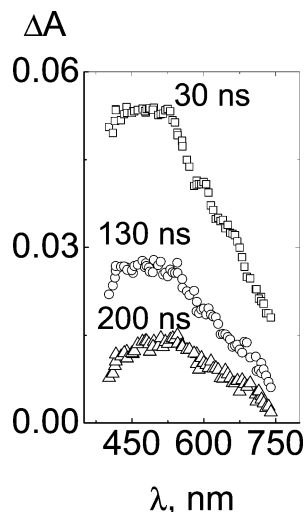
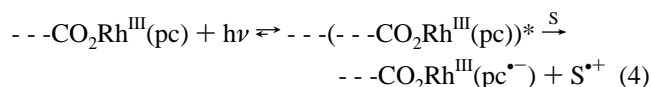


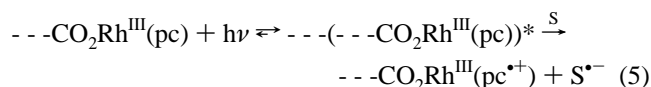
Figure 6. Photogenerated transient spectra recorded when deaerated solutions of poly-Rh^{III}(pc), 2.4×10^{-4} M in $- - -\text{CO}_2\text{Rh}^{\text{III}}(\text{pc})$ pendants, were flash irradiated at 351 nm.

spectrum. This component of the luminescence was not previously observed with $\text{XRh}^{\text{III}}(\text{pc})$ ($\text{X} = \text{Cl}, \text{Br}, \text{I}$). In addition, a fast decaying component of the emission, $t < 20$ ns, exhibited a maximum at ~ 440 nm. It was assigned to the radiative relaxation of the second $^1\pi\pi^*$ excited state. This is the same anti-Kasha emission previously communicated for $\text{XRh}^{\text{III}}(\text{pc})$ ($\text{X} = \text{Cl}, \text{Br}, \text{I}$).²⁶

The spectra of the pendent ligand radicals, $- - -\text{CO}_2\text{Rh}^{\text{III}}(\text{pc}^{\bullet-})$ or $- - -\text{CO}_2\text{Rh}^{\text{III}}(\text{pc}^{\bullet+})$, were recorded in flash photochemical experiments where poly-Rh^{III}(pc), were flash irradiated in solutions containing 2.4×10^{-4} M $- - -\text{CO}_2\text{Rh}^{\text{III}}(\text{pc})$ pendants and either an electron donor or an electron acceptor, eq 4 and 5.



S = TEA or TEOA



S = MV^{2+} or $\text{Fe}^{\text{III}}(\text{py}[14]\text{dieneN}_4)^{3+}$

The various concentrations used in the reduction, eq 4, and oxidation, eq 5, of the excited state were 1 M TEA (TEA = triethylamine); 0.1, 0.4, and 1.0 M TEOA (TEOA = 2,2',2''-triethanolamine); 10^{-2} M MV^{2+} (MV^{2+} = methyl viologen); and 10^{-4} M $\text{Fe}^{\text{III}}(\text{py}[14]\text{dieneN}_4)^{3+}$.

In contrast to the reactions of the polymer with pulse radiolytically generated radicals, the formation of $- - -\text{CO}_2\text{Rh}^{\text{III}}(\text{pc}^{\bullet-})$ and $- - -\text{CO}_2\text{Rh}^{\text{III}}(\text{pc}^{\bullet+})$ occurred in a time scale, $t = 10^2$ ns. These rates were fast by comparison to those of the reactions between poly-Rh^{III}(pc) and pulse radiolytically generated radicals. The difference was attributed to the presence of the electron donor or acceptor S near the electronically excited pendants, $(- - -\text{CO}_2\text{Rh}^{\text{III}}(\text{pc}))^*$, in the photochemical processes. Back electron-transfer reactions were observed in a time scale, $t > 10^2$ ns. These processes exhibited second-order kinetics. In Table 1, $k/\Delta\epsilon$ is the ratio of the second-order rate constant to the difference, $\Delta\epsilon$, between the extinction coefficients of the radicals and the polymer. It was calculated at wavelengths of the maximum in the difference spectrum of $- - -\text{CO}_2\text{Rh}^{\text{III}}(\text{pc}^{\bullet-})$ or $- - -\text{CO}_2\text{Rh}^{\text{III}}(\text{pc}^{\bullet+})$. Since the pulse radiolytic experiments yield

Table 1. Ratio of the Rate Constant to the Difference of Extinction Coefficient, $k/\Delta\epsilon$, of the Coordinated pc Radical at 470 nm^a

reaction	$k/\Delta\epsilon$, cm s ⁻¹
$\text{TEA}^+ + - - -\text{CO}_2\text{Rh}^{\text{III}}(\text{pc}^{\bullet-}) \rightarrow \text{TEA} + - - -\text{CO}_2\text{Rh}^{\text{III}}(\text{pc})$	1.3×10^8
$\text{TEOA}^+ + - - -\text{CO}_2\text{Rh}^{\text{III}}(\text{pc}^{\bullet-}) \rightarrow \text{TEOA} + - - -\text{CO}_2\text{Rh}^{\text{III}}(\text{pc})$	2.4×10^8
$\text{MV}^{\bullet+} + - - -\text{CO}_2\text{Rh}^{\text{III}}(\text{pc}^{\bullet+}) \rightarrow \text{MV}^{2+} + - - -\text{CO}_2\text{Rh}^{\text{III}}(\text{pc})$	4.5×10^8
$\text{Fe}^{\text{II}}(\text{py}[14]\text{dieneN}_4)^{2+} + - - -\text{CO}_2\text{Rh}^{\text{III}}(\text{pc}^{\bullet+}) \rightarrow \text{Fe}^{\text{III}}(\text{py}[14]\text{dieneN}_4)^{3+} + - - -\text{CO}_2\text{Rh}^{\text{III}}(\text{pc})$	2.7×10^8

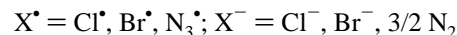
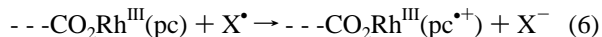
^a The rate constant is for the back-electron-transfer reaction of the photooxidized or photoreduced $- - -\text{CO}_2\text{Rh}^{\text{III}}(\text{pc})$ pendants.

an approximate value for the difference of extinction coefficients, $\Delta\epsilon \sim 10^3 \text{ M}^{-1} \text{ cm}^{-1}$, the second-order rate constants calculated with values of $k/\Delta\epsilon$ in Table 1 must have a $10^{11} \text{ M}^{-1} \text{ s}^{-1}$ order of magnitude.

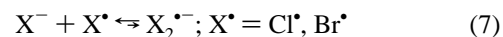
Discussion

The UV-vis spectroscopy of poly-Rh^{III}(pc) shows a large fraction of $- - -\text{CO}_2\text{Rh}^{\text{III}}(\text{pc})$ pendants forming stacks in the strand of poly(acrylate) polymer. A similar stacking has not been observed in homogeneous solutions of $\text{XRh}^{\text{III}}(\text{pc})$ ($\text{X} = \text{Cl}, \text{Br}, \text{I}$), and it must be regarded as an intrinsic phenomenon of the poly-Rh^{III}(pc). The stacks of $- - -\text{CO}_2\text{Rh}^{\text{III}}(\text{pc})$ pendants are likely to be located inside the spherules observed in the AFM microscope. This distribution of the pendants in the strand of polymer is favored by the hydrophobic character of $- - -\text{CO}_2\text{Rh}^{\text{III}}(\text{pc})$ pendants; i.e., it will isolate them inside the spherules from the aqueous media. Constrained to the small volume of the spherules, the $- - -\text{CO}_2\text{Rh}^{\text{III}}(\text{pc})$ pendants achieve local concentrations far larger than those of the $\text{XRh}^{\text{III}}(\text{pc})$ ($\text{X} = \text{Cl}, \text{Br}, \text{I}$) complexes in homogeneous solution, a condition also favoring the formation of stacks. Bonding between $- - -\text{CO}_2\text{Rh}^{\text{III}}(\text{pc})$ pendants in the stacks must also be responsible of the persistence for the hypercoiled morphology when carboxylate pendants, not coordinated to Rh^{III}(pc), are deprotonated at pH > 6. Indeed, the bonding between $- - -\text{CO}_2\text{Rh}^{\text{III}}(\text{pc})$ pendants in a stack is, to a large extent, pH independent. In acidic media, e.g., pH = 6, the H-bonds from the protonated carboxylates could make an additional contribution to the hypercoiled structure of poly-Rh^{III}(pc).

Hypercoiling and Redox Reactions. The hypercoiled structure of poly-Rh^{III}(pc) accounts for the diverse redox behavior of the polymer. Oxidation of the $- - -\text{CO}_2\text{Rh}^{\text{III}}(\text{pc})$ pendants is most likely to be carried out in the spherules by neutral X[•] radicals, eq 6

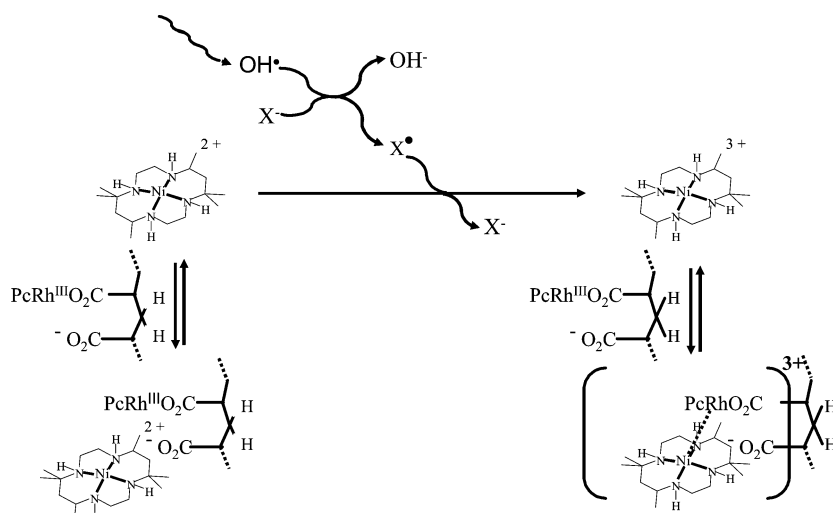


that are hydrophobic in nature and exist in equilibrium with the spectroscopically observable $\text{X}_2^{\bullet-}$ anion radicals, eq 7.

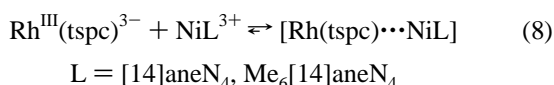


Reactions of the larger hydrophilic anion radicals with $- - -\text{CO}_2\text{Rh}^{\text{III}}(\text{pc})$ pendants are expected to be kinetically disfavored by electrostatic interactions and the hydrophobic environment hosting the stacks. In contrast to the $- - -\text{CO}_2\text{Rh}^{\text{III}}(\text{pc}^{\bullet+})$ radical produced in eq 6, the reactions of poly-Rh^{III}(pc) or Rh^{III}(tspc)³⁻ with Ni(III) macrocyclic complexes gave products with a spectrum having a band at ~ 530 nm and no bleach of the ~ 675 nm pc's or tspc's Q-band. The spectrum is devoid, therefore, of the characteristic features of the radical's spectrum. On the basis of this spectroscopic features, the

Scheme 1



products must be assigned as adducts of the Ni(III) complex with $\text{Rh}^{\text{III}}(\text{tspc})^{3-}$ or $-\text{CO}_2\text{Rh}^{\text{III}}(\text{pc})$ pendants in poly- $\text{Rh}^{\text{III}}(\text{pc})$. A single equilibrium, eq 8



accounts for the spectral changes observed in the reaction of $\text{Rh}^{\text{III}}(\text{tspc})^{3-}$ with NiL^{3+} to form the adduct $[\text{Rh}^{\text{III}}(\text{tspc})\cdots\text{NiL}]$.

The mechanism of the reaction of NiL^{3+} with poly- $\text{Rh}^{\text{III}}(\text{pc})$ is more complex than eq 8. It must first involve the coordination of NiL^{2+} and NiL^{3+} to carboxylates not bonded to $\text{Rh}^{\text{III}}(\text{pc})$ by a process similar to the one observed with the unreactive UO_2^{2+} , Figure 2. Coordination of the Ni macrocycles to the strand of polymer makes the formation of the adduct more than 1 order of magnitude faster, i.e., 10^6 s^{-1} vs 10^5 s^{-1} , than eq 8. In a summarized manner, the processes initiated with $\text{Ni}^{\text{II}}(\text{Me}_6[\text{14}] \text{aneN}_4)^{2+}$ oxidation and formation of the adduct are described in Scheme 1, where radiolytically generated OH^\bullet radicals oxidize X = Cl^- or Br^- to produce radicals X^\bullet . The radical X^\bullet oxidize $\text{Ni}^{\text{II}}(\text{Me}_6[\text{14}] \text{aneN}_4)^{2+}$ which will form the corresponding adducts with pendant $-\text{CO}_2\text{Rh}^{\text{III}}(\text{pc})$.

Modeling of the overall reaction between $(\text{CH}_3)_2\text{C}^\bullet\text{OH}$ radicals and $-\text{CO}_2\text{Rh}^{\text{III}}(\text{pc})$ was made on the assumption of different contributions from the reaction of the radicals with the dimers to form $-\text{CO}_2\text{Rh}^{\text{III}}(\text{pc}^\bullet)$ radicals and monomeric $-\text{CO}_2\text{Rh}^{\text{III}}(\text{pc})$, eq 3. The model providing the best agreement with the time-resolved bleach of the Q-band at $\sim 650 \text{ nm}$ and the formation of the $-\text{CO}_2\text{Rh}^{\text{III}}(\text{pc}^\bullet)$ radical absorption at $\sim 500 \text{ nm}$, Figure 7a, suggests a significant participation of the dimers in the overall reaction, eqs 2 and 3. If the reaction of the dimers with the radical is diminished or ignored altogether, the bleach of the monomer's Q-band became too large in relationship to the absorption of the $-\text{CO}_2\text{Rh}^{\text{III}}(\text{pc}^\bullet)$ radical, Figure 7b. In the other limit, a contribution too large from the dimer's reaction, eq 3, gives an absorbance growth at $\sim 650 \text{ nm}$, Figure 7c. This new absorption band results from an overestimated generation of $-\text{CO}_2\text{Rh}^{\text{III}}(\text{pc})$ monomer which has a much larger extinction coefficient at $\sim 630 \text{ nm}$ than the $(-\text{CO}_2\text{Rh}^{\text{III}}(\text{pc}))_2$ dimer. The best fit of the spectral changes yields rate constants $k = 5.0 \times 10^9 \text{ M}^{-1} \text{ s}^{-1}$ for eq 2 and $k = 8.0 \times 10^8 \text{ M}^{-1} \text{ s}^{-1}$ for eq 3.

Hypercoiling and Excited-State Processes. In aqueous solution, stacks of $-\text{CO}_2\text{Rh}^{\text{III}}(\text{pc})$ pendants in hydrophobic pockets of the strand account for differences among the

photophysical processes of the pendants and those previously communicated for $\text{XRh}^{\text{III}}(\text{pc})$ ($\text{X} = \text{Cl}, \text{Br}, \text{I}$). These differences are shown in Figure 8. The most marked difference is the photogeneration of an excited state with the spectrum and lifetime of a ligand field, LF, excited-state not observed when

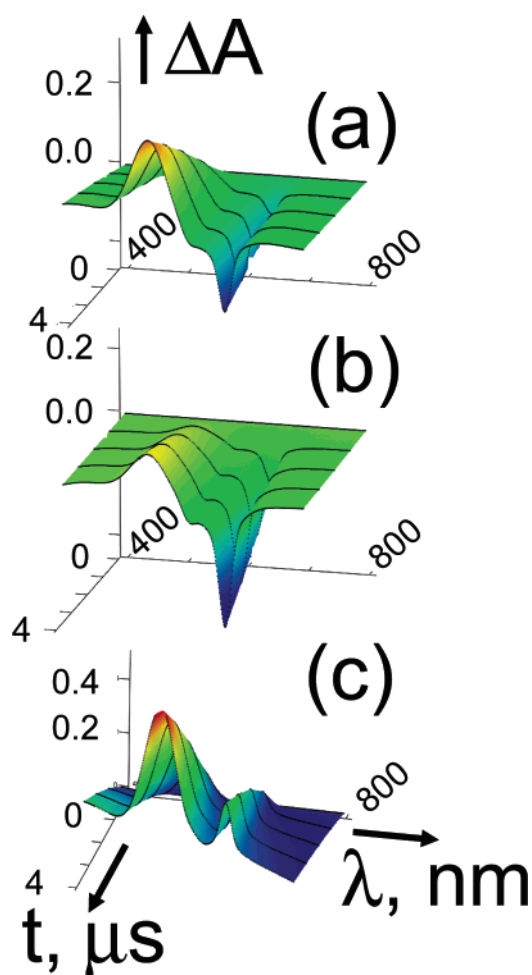


Figure 7. Model of the spectral changes caused by reactions of $(\text{CH}_3)_2\text{C}^\bullet\text{OH}$ radicals with monomeric and dimeric $-\text{CO}_2\text{Rh}^{\text{III}}(\text{pc})$ pendants. A rate constant, $k = 5 \times 10^9 \text{ s}^{-1}$, was used for the reaction of $(\text{CH}_3)_2\text{C}^\bullet\text{OH}$ radicals with monomeric $-\text{CO}_2\text{Rh}^{\text{III}}(\text{pc})$ pendants. The rate constant used for the reaction of $(\text{CH}_3)_2\text{C}^\bullet\text{OH}$ radicals with $(-\text{CO}_2\text{Rh}^{\text{III}}(\text{pc}))_2$ pendants is: $1 \times 10^6 \text{ M}^{-1} \text{ s}^{-1}$ (a), $8 \times 10^8 \text{ M}^{-1} \text{ s}^{-1}$ (b), and $3 \times 10^9 \text{ M}^{-1} \text{ s}^{-1}$ (c).

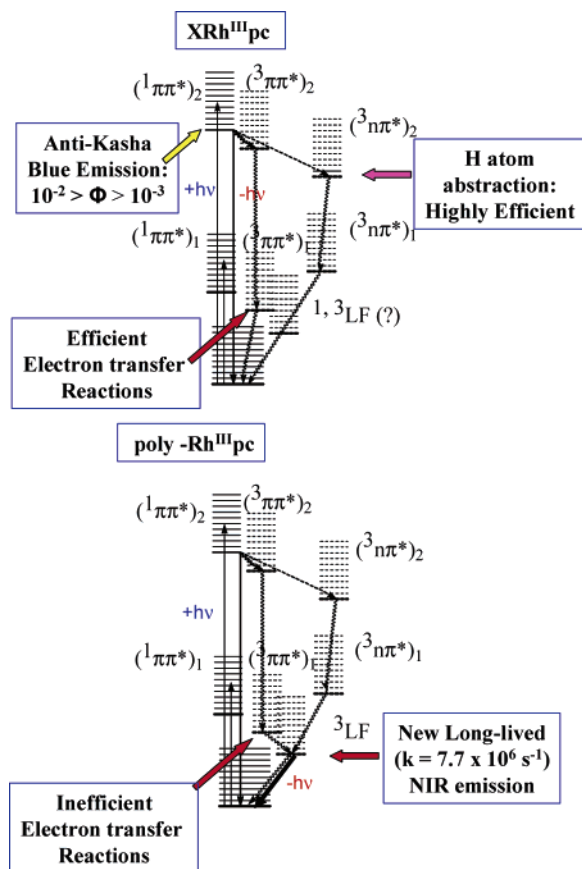
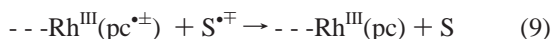


Figure 8. Comparison of the Jablonsky energy diagrams for monomeric $\text{XRh}^{\text{III}}(\text{pc})$, top, and $-\text{CO}_2\text{Rh}^{\text{III}}(\text{pc})$ pendants in poly- $\text{Rh}^{\text{III}}(\text{pc})$, bottom. The question mark in the top diagram shows where LF excited states of $\text{Rh}(\text{III})$ could be expected to be in the $\text{XRh}^{\text{III}}(\text{pc})$ monomer.

$\text{XRh}^{\text{III}}(\text{pc})$ complexes were irradiated in homogeneous solution. In addition the efficiency of the lowest phthalocyanine-centered excited state, $(^3\pi\pi^*)_1$, to undergo electron-transfer reactions is decreased in relation to similar reactions of the $(^3\pi\pi^*)_1$ in $\text{XRh}^{\text{III}}(\text{pc})$. The decrease in the efficiency $(^3\pi\pi^*)_1$ to undergo electron-transfer reactions can be related to the $(^3\pi\pi^*)_1$ to ^3LF conversion in poly- $\text{Rh}^{\text{III}}(\text{pc})$, a process that was not previously observed in the photophysics of $\text{XRh}^{\text{III}}(\text{pc})$.



Although the electron-transfer processes of the $(^3\pi\pi^*)_1$ with electron donors or acceptors is inefficient, the formation products, eqs 1 and 2, and the back-electron-transfer reactions of the phthalocyanine radicals, eq 9, were followed by means of the intense absorbance change at wavelengths of the Q-band. The reactions depicted in eq 9 occur with faster rates, rate constants $k = 10^{11} \text{ M}^{-1} \text{ s}^{-1}$, than those of related reactions between the $\text{XRh}^{\text{III}}(\text{pc}^{\pm})$ and S^{\mp} radicals, rate constants $k = 10^7$ or $10^8 \text{ M}^{-1} \text{ s}^{-1}$. The faster rates suggest that the radicals S^{\mp} are not able to diffuse too far into the bulk of the solution before they react back with the $-\text{CO}_2\text{Rh}^{\text{III}}(\text{pc}^{\pm})$ radicals in the strand of polymer.

Conclusions

In relation to poly(acrylate), the phthalocyanine pendants play an important stabilizing role in the strand's hypercoiled morphology. Environmental conditions created by the hypercoiling change the thermal and photochemical reactivity of pendent $-\text{CO}_2\text{Rh}^{\text{III}}(\text{pc})$ groups. To a large extent, these changes in the reactivity of the $-\text{CO}_2\text{Rh}^{\text{III}}(\text{pc})$ pendants appear to be the

dual result of the medium and steric effects. They can be associated with a large number of pendants inside the spherules of the hypercoiled strand and placed, therefore, in a medium much different from the bulk of the solution.

Acknowledgment. The work described herein was supported by the Office of Basic Energy Sciences, of the US Department of Energy. This is Contribution No. NDRL-4668 from the Notre Dame Radiation Laboratory.

References and Notes

- (1) Haywood-Small, S. L.; Vernon, D. I.; Griffiths, J.; Schofield, J.; Brown, S. B. *Biochem. Biophys. Res. Commun.* **2006**, *339*, 569.
- (2) Tzekov, R.; Lin, T.; Zhang, K. M.; Jackson, B.; Oyejide, A.; Orilla, W.; Kulkarni, A. D.; Kuppermann, B. D.; Wheeler, L.; Burke, J. *Invest. Ophthalmol. Visual Sci.* **2006**, *47*, 377.
- (3) Gurek, A. G.; Basova, T.; Luneau, D.; Lebrun, C.; Kol'tsov, E.; Hassan, A. K.; Ahsen, V. *Inorg. Chem.* **2006**, *45*, 1667.
- (4) Hasegawa, H.; Ueda, R.; Kubota, T.; Mashiko, S. *Thin Solid Films* **2006**, *499*, 289.
- (5) Yang, L. F.; Guan, M.; Bian, Z. Q.; Xie, J. Q.; Chen, T. P.; Huang, C. H. *Thin Solid Films* **2006**, *500*, 224.
- (6) Generosi, A.; Paci, B.; Albertini, V. R.; Perfetti, P.; Paoletti, A. M.; Pennesi, G.; Rossi, G.; Caminiti, R. *J. Appl. Phys.* **2006**, *99*, Art. No. 044901.
- (7) Mortimer, R. J.; Dyer, A. L.; Mayer, I.; Nunes, G. S.; Toma, H. E.; Araki, K. E. *J. Inorg. Chem.* **2006**, 850.
- (8) Kitamura, Y.; Mifune, M.; Hino, D.; Yokotani, S.; Saito, M.; Tsukamoto, I.; Iwado, A.; Saito, Y. *Talanta* **2006**, *69*, 43.
- (9) Kostka, M.; Zimcik, P.; Miletin, M.; Klemra, P.; Kopecky, K.; Musil, Z. *J. Photochem. Photobiol. A* **2006**, 178.
- (10) Rajendiran, N.; Santhanalakshmi, J. *J. Mol. Catal. A* **2006**, *245*, 185.
- (11) Ballesteros, B.; de la Torre, G.; Torres, T.; Hug, G. L.; Rahman, G. M. A.; Guldi, D. M. *Tetrahedron* **2006**, *62*, 2097.
- (12) De Feyter, S.; De Schryver, F. *Supermolecular Dye Chemistry. Top. Cur. Chem.* **2005**, *258*, 205.
- (13) Wrobel, D.; Dudkowiak, A. *Mol. Cryst. Liq. Cryst.* **2006**, *448*, 15.
- (14) Christendat, D.; David, M. A.; Morin, S.; Lever, A. B. P.; Kadish, K. M.; Shao, J. G. *J. Porphyrins Phthalocyanines* **2005**, *9*, 626.
- (15) Wöhrle, D. *Macromol. Rapid Commun.* **2001**, *22*, 68.
- (16) Magaraggia, M.; Visona, A.; Furlan, A.; Pagnan, A.; Miotto, G.; Tognon, G.; Jori, G. *J. Photochem. Photobiol. B* **2006**, *82*, 53.
- (17) Karandikar, P.; Chandwadkar, A. J.; Agashe, M.; Ramgir, N. S.; Sivasanker, S. *Appl. Catal. A* **2006**, *297*, 220.
- (18) Tome, J. P. C.; Pereira, A. M. V. M.; Alonso, C. M. A.; Neves, M. G. P. M. S. A.; Tome, C.; Silva, A. M. S.; Cavaleiro, J. A. S.; Martinez-Diaz, M. V.; Torres, T.; Rahman, G. M. A.; Guldi, D. M. *Eur. J. Org. Chem.* **2005**, 257.
- (19) Zhang, Y.; Sun, X.; Niu, Y.; Xu, R.; Wang, G.; Jiang, Z. *Polymer* **2006**, *47*, 1569.
- (20) McKeown, N. B. *J. Mater. Chem.* **2000**, *10*, 1979.
- (21) Meisel, P.; Kocher, T. *J. Photochem. Photobiol. B* **2005**, *79*, 159.
- (22) Naik, R.; Joshi, P.; Deshpande, R. K. *Catal. Commun.* **2004**, *5*, 195.
- (23) I. Manners *Science* **2001**, *294*, 1664.
- (24) Wöhrle, D. In *Phthalocyanines. Properties and applications*; Leznoff, C. C., Lever, A. B. P., Eds.; VCH: New York, 1989; Chapter 2.
- (25) Muralidharan, S.; Ferraudi, G.; Schmatz, K. *Inorg. Chem.* **1982**, *21*, 2961.
- (26) Ferraudi, G.; Muralidharan, S. *Inorg. Chem.* **1983**, *22*, 1369.
- (27) Ferraudi, G. In *Phthalocyanines. Properties and applications*; Leznoff, C. C., Lever, A. B. P., Eds.; VCH: New York, 1989; Chapter 4, and references therein.
- (28) De Witt, D. G. *Coord. Chem. Rev.* **1996**, *147*, 209.
- (29) Wang, X.-Y.; Prabhu, R. N.; Schmehl, R. H.; Weck, M. *Macromolecules* **2006**, *39*, 3140.
- (30) Guerrero, J.; Piro, O. E.; Wolcan, E.; Feliz, M. R.; Ferraudi, G.; Moya, S. A. *Organometallics* **2001**, *20*, 2842.
- (31) Hugh, G. L.; Wang, Y.; Schöneich, C.; Jiang, P.-Y.; Fesenden, R. W. *Radiat. Phys. Chem.* **1999**, *54*, 559.
- (32) Feliz, M. R.; Ferraudi, G. *Inorg. Chem.* **1998**, *37*, 2806.
- (33) Buxton, G. V.; Greenstock, C. L.; Hellman, W. P.; Ross, A. B.; Tsang, W. J. *Phys. Chem. Ref. Data* **1988**, *17*, 513.
- (34) Getoff, N.; Ritter, A.; Schworer, F. *Radiat. Phys. Chem.* **1993**, *41*, 797.
- (35) Dutta, S. K.; Ferraudi, G. *J. Phys. Chem. A* **2001**, *105*, 4241.
- (36) Gnignino, K. P. Tan, K. L. In *Polymer photophysics*; Phillips, D., Ed.; Chapman and Hall: New York, 1985; Chapter 7, and references therein.
- (37) Sheiko, S. S. *Adv. Polym. Sci.* **2000**, *151*, 61.